

## Co-transport-induced instability of membrane voltage in tip-growing cells

M. Leonetti, P. Maroq, and J. Nuebler

IRPHE, Universit s Aix-Marseille I and II, UMR CNRS 6594,  
Technop le de Ch teau-Gombert, 13384 Marseille Cedex 13, France

F. Homble

Laboratory for Structure and Function of Biological Membranes,  
Universit  Libre de Bruxelles, CP 206/2, Campus Plaine, B-1050 Brussels, Belgium  
(Dated: September 23, 2005)

A salient feature of stationary patterns in tip-growing cells is the key role played by the symports and antiports, membrane proteins that translocate two ionic species at the same time. It is shown that these co-transporters destabilize generically the membrane voltage if the two translocated ions diffuse differently and carry a charge of opposite (same) sign for symports (antiports). Orders of magnitude obtained for the time and lengthscale are in agreement with experiments. A weakly nonlinear analysis characterizes the bifurcation.

PACS numbers: 87.10.+e, 05.65.+b, 87.16.Jv

Spatiotemporal pattern formation of the electric membrane potential in cells and tissues emerges from collective dynamics and activity of membrane ion channels. Action potential and cardiac excitation spiral waves are paradigmatic examples of nonstationary pattern formation [1, 2]. Stationary patterns of ionic currents are widespread in fungi, plant cells (algae for example), protozoa and insects: *Chara corallina*, *Fucus zygote* and *Achlya* are the model cells [3, 4]. Such patterns are correlated to cell polarization, apical growth, morphogenesis and nutrient acquisition. The characteristic wavelengths and times vary from a few millimeters to ten microns and from one hour to one minute, respectively. These times correspond typically to a membrane protein or an ion diffusive time. Two mechanisms have been proposed [5]: one based on the electromigration of membrane proteins [6, 7, 8, 9, 10] and the other resulting from a negative differential conductance characterizing voltage-gated channels [11, 12, 13].

However, the origin of current patterns is still unclear in tip-growing cells where transcellular currents are mainly produced by the pump and a co-transporter, a membrane carrier that translocates two species of ions at the same time [14, 15] (see Fig. 1). Three points of view are proposed by biologists for tip-growing cells: ionic currents may be a consequence of cellular growth, a self-organized pattern coupled to growth or, alternatively, arise as a self-organized pattern which precedes cellular growth [16]. The appearance of a lateral branching preceded by an inward current supports the hypothesis of self-organization in *Achlya* [15]. The mechanisms proposed in the literature cannot explain such patterns [17].

In this letter, we ask the broader question: how does the stability of the membrane voltage depend on co-transporters? Only the contribution of channels to membrane voltage instability has been investigated in the literature. We demonstrate here that the voltage along a membrane containing co-transporters is linearly unstable

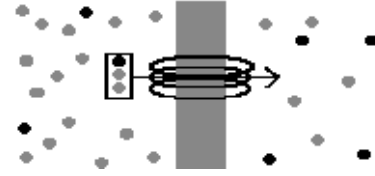


FIG. 1: The pump (not drawn) generates a gradient of the electrochemical potential through the membrane by translocating continuously one species of ions (grey disk). This stored free energy is used by the symport, a co-transporter, to transfer a second species of ion (black disk) or nutrient against its own gradient if necessary. The stoichiometry of the drawn symport is equal to 2: two grey disks for one black disk.

on a diffusive (not electrical) characteristic time. The stationary pattern is a stationary modulation of ionic concentrations, membrane voltage and transcellular ionic currents. The mechanism is specific to this kind of carriers since each ionic transporter is characterized by a positive differential conductance.

Consider two ions 1, 2 of valence numbers  $z_j$  and concentrations  $C_j$ , diffusing along a cylindrical cellular membrane of radius  $r$ . As in the cable model, the electrodynamics is governed by a one-dimensional electrodiffusive equation for each ion:

$$\partial_t C_j = D_j \partial_x^2 C_j + z_j (e D_j = k_B T) \partial_x (C_j \partial_x V) - (2=r) J_j \quad (1)$$

and the capacitive relation for the membrane voltage  $V$ :

$$V = V_0 + (F r = 2 C_m) (z_1 (C_1 - C_{10}) + z_2 (C_2 - C_{20})) \quad (2)$$

where  $D_j$  is the diffusion coefficient of ion  $j$ ,  $V_0$  the resting membrane potential ( $-0.1$  V),  $C_m$  the specific membrane capacitance ( $0.01$  Fm<sup>-2</sup>) and  $C_{j0}$  the concentration of ion  $j$  in the resting state. The standard cable model is recovered simply from (1-2) when all ionic diffusion coefficients are identical. In our model, the

uxes  $J_j$  take into account the intracellular chemical reactions as well as the membrane fluxes through pumps, co-transporters, channels and uniports. The pump uses chemical energy (ATP) to translocate ions from one side to the other (the 1-ion in this Letter), generating an electrochemical potential gradient through the membrane: for example,  $H^+$ -ATPase in plant cells. Consequently, the 1-ion is a cation. Co-transporters use this stored free molar energy to transfer one 2-ion for  $n$  1-ions in the same (opposite) sense for the symport (antiport) carrier (see Fig. 1). In practice, the stoichiometry  $n$  is equal to either 1 or 2. In tip-growing cells, the 2-ion is often an essential nutrient for future vegetative metabolism and consequently, implied in many chemical processes based on enzymatic binding reactions: metabolism in *Alchya hyphae* with the methionine (an amino acid) uptake or the carbon dioxide supply to chloroplasts for photosynthesis in *Chara corallina* by  $HCO_3^-$  entry. Finally, the flux  $J_j$  of each ion  $j$  is:

$$J_1 = J_{pch} + nJ_s; \quad (3)$$

$$J_2 = J_s + C_2 + J_2^{NL} \quad (4)$$

where  $J_{pch}$  is the flux through active pumps and passive channels translocating the 1-ion,  $J_s$  ( $nJ_s$ ) is the flux of the 2-ion (1-ion) through the co-transporter, and  $J_2^{NL}$  is the (concentration-dependent) nonlinear part of  $J_2$ , due to intracellular chemical processes. The mechanism of the (linear) voltage instability does not depend on the functional form of  $J_2^{NL}$ . The characteristic kinetic constant of nutrient uptake is necessarily positive. The sign is + for a symport and - for an antiport. In the following, we consider the case of the symport but the extension to that of the antiport is straightforward. For simplicity's sake,  $J_{pch}$  and  $J_s$  do not depend on concentrations and vary linearly with the membrane potential  $V$ , characterized by their positive conductances:  $G_{pch} = z_1 F$  ( $@J_{pch}=@V$ ) and  $G_s = z_1 F$  ( $@J_s=@V$ ). Even if a co-transporter is often called a secondary active carrier, its working is passive. Consequently, the differential conductance of the current through the co-transporter,  $(n + z_2=z_1)G_s$  is always positive (positive Onsager coefficient). Then, there is no local positive feedback provided by protein characteristics. In the homogeneous resting state,  $J_j = 0$  for each ion: the molar flux  $J_{s0}$  of the nutrient uptake in the resting state may be nonzero. Equations (1-4) are scaled with dimensionless coordinates for space  $x^0 = x =$  and time  $t^0 = t =$  with the cable length characteristic of the pumps and channels (primaries are then dropped for simplicity),  $\tau^2 = r = 2G_{pch}$  and the diffusive time  $\tau^2 = D^{-2} = D_1 D_2$ , where  $\tau$  is the bulk ionic conductivity and  $D = \frac{1}{2}(D_1 + D_2)$  is the mean coefficient of diffusion. We set  $j = z_j^2 C_{j0} = (z_1^2 C_{10} + z_2^2 C_{20})$  equal to 0.5 in all the following.

The control parameter is the positive conductance ratio,  $\gamma = G_s/G_{pch}$  that controls the ionic membrane fluxes. The stability of the homogeneous equilibrium state is analyzed by considering the evolution of actual

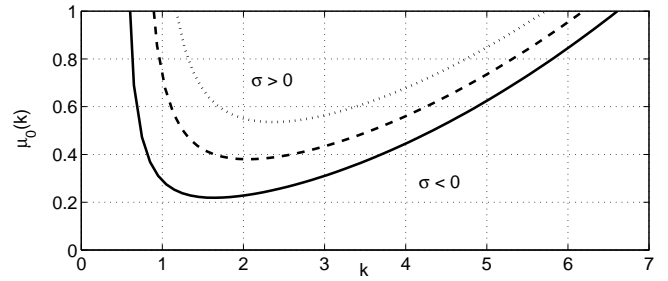


FIG. 2: The neutral curve  $\mu_0(k)$  is defined by  $(\mu_0(k); k) = 0$  and has a minimum at  $(k_c; \mu_c)$ . Above the critical control parameter  $\mu_c$ , the membrane voltage is unstable. Parameters are:  $n = 2$ ,  $z_1 = 1$ ,  $z_2 = -1$ ,  $D_1 = 10^{-5} \text{ cm}^2 \text{ s}^{-1}$ ,  $D_2 = 10^{-7} \text{ cm}^2 \text{ s}^{-1}$  (common for the three neutral curves), and  $\gamma_1 = 0.1$  (—),  $\gamma_1 = 0.2$  (---) and  $\gamma_1 = 0.3$  (···).

tions of voltage  $V$  and ionic concentrations  $C_j$  and consequently, the linearized equations of (1-4):  $H(x;t) = H_0 e^{st + ikx}$  where  $k$  is the wave number of the perturbation and  $H$  refers to  $V$  and  $C_j$ . Two real solutions for  $s = s(k)$  are determined:  $\text{Im}(s) = 0$ ,  $\text{Re}(s) = \mu(k)$ . The first one is the well-known fast capacitive relaxation. The second one yields the growth rate of the instability:

$$\mu(k) = \frac{k^4 + \frac{D}{D_1} k^2 + 1 + \frac{n + \frac{D_1 z_2}{D_2 z_1}}{k^2 + 1 + (n + z_2=z_1)}}{\frac{1}{D_2} \frac{(D - D_2)k^2 + (D_1 - D_2)(1 + n)}{k^2 + 1 + (n + z_2=z_1)} + \frac{D}{D_1}} \quad (5)$$

where  $\gamma_1 = \gamma G_{pch} (D_1 - D_2)$  is dimensionless. Since the capacitance does not appear in (5), this characteristic (inverse) time is diffusive. From  $(\mu_0(k); k) = 0$ , the neutral curve  $\mu_0(k)$  is determined and has a minimum defining the critical values of the control parameter  $\mu_c$  and the wavenumber  $k_c$  (Fig. 2):

$$\mu_c = \frac{D_1 D_2}{D^2 (z_2 D_1 = z_1 + n D_2)} \left( 2k_c^2 + \frac{D}{D_1} + \gamma_1 \left( \frac{D}{D_2} - 1 \right) \right) \quad !$$

$$(k_c^2 - k_0^2)^2 = k_0^4 + \frac{1}{D_1 D_2} (D_1 - D_2) + k_0^2 \left( \frac{D}{D_1} + \gamma_1 \left( \frac{D}{D_2} - 1 \right) \right) \quad !$$

where  $k_0^2 = \frac{n - \gamma_1 (D_1 - D_2)}{(z_2 D_1 = z_1 + n D_2)}$ . The particular case  $\gamma_1 = 0$  corresponds to a long-wavelength instability ( $k_c = 0$ ), and will not be treated here [9].

For  $\gamma > \gamma_c > 0$ , the growth rate is positive in a finite range of wavenumbers. The limit case of small binding reactions may help clarify the nature of this instability. For small but nonzero  $\gamma_1$ , the homogeneous resting state is unstable ( $\mu > 0$ ) against spatial perturbations if  $1 + (n + D_1 z_2 = D_2 z_1) < 0$ . Recalling that  $0 < n + z_2=z_1$ , two necessary conditions for instability are  $D_1 > n D_2 \frac{z_1}{z_2}$  and  $z_2=z_1 < 0$  [18]. The former is generally verified since binding reactions reduce notably

the effective diffusion of the 2-ion [19]; the latter is fulfilled for the symports  $H^+ = HCO_3^-$  in *Chara corallina* and  $H^+$  - methionine in *Achlya*. For large control parameter and small  $\lambda_1$ , the wavelength  $\lambda_p$  of the pattern satisfies:  $\lambda_p \approx 2 \sqrt{r D_2 / 2 G_s D'}^{1/2} \approx \lambda_{cable} (D_2 / D')^{1/2}$  where  $\lambda_{cable}$  is provided by the cable model and may be experimentally measured by two impaled electrodes. An order of magnitude of  $\lambda_p$  can thus be evaluated. In *Achlya* hyphae, some measurements indicate  $\lambda_{cable} \approx 2$  mm [20]. On the basis of measurements of the effective diffusion of the calcium ion, a reasonable value for the diffusion coefficient of the 2-ion is  $D_2 \approx 10^{-7} \text{ cm}^2/\text{s}$ . We thus expect a characteristic pattern wavelength  $\lambda_p \approx 100 \mu\text{m}$ , in agreement with experiments. The characteristic time  $\tau_p$  required to produce the pattern is of the order of a diffusive time:  $\tau_p \approx \lambda_p^2 / D_2$ , dominated by the slower ionic diffusion. Using the previous values, we find  $\tau_p \approx 10^3 \text{ s}$ , in agreement with experiments on *Achlya* hyphae [3].

Equations (1-4) have been solved numerically for a large range of parameters to confirm the previous results. For simplicity, the nonlinear flux  $J_2^{NL}$  is given by a truncated expansion in powers of the concentration of the 2-ion:

$$J_2^{NL} = C_{20} \sum_{j=2;3}^X j (C_2 - C_{20}) = C_{20}^j \quad (6)$$

This form generalizes the expansion of a Michaelis-Menten enzyme kinetics term in the limit of large Michaelis constant: our goal is to take into account at a phenomenological level some of the complexity due to the function of the 2-ion. The coefficient  $\beta_3$  must be positive to ensure nonlinear convergence. The simulation depends on two additional dimensionless parameters:  $\beta_2 = \frac{1}{2} \frac{J_0}{J_2} = \frac{1}{2} \frac{(z_2 F G_{pch} C_{20} (D_1 - D_2)^2)}{(z_2 F)^2 G_{pch} C_{20}^2 (D_1 - D_2)^3}$  and  $\beta_3 = \frac{1}{3} \frac{J_0}{J_2} = \frac{1}{3} \frac{(z_2 F)^2 G_{pch} C_{20}^2 (D_1 - D_2)^3)}{(z_2 F)^2 G_{pch} C_{20}^2 (D_1 - D_2)^3}$ . Generally, the voltage relaxes to zero on a characteristic capacitive time, as expected from the cable model. However, for relevant parameters characterizing a symport, a cellular pattern of voltage and concentrations appears after a transient whose duration is of the order of magnitude of the diffusive time  $\tau_p$  (Fig. 3). Outer and inner transcellular currents flow periodically through the membrane. It has been established that the ohmic part  $I_{ohm}$  of the dimensionless extracellular current normal to the membrane is given by the relation:  $I_{ohm} = D' (I_1 = D_1 + I_2 = D_2) = G_{pch} J_0 j$  [12]. An outer (inner) ohmic current corresponds to an hyperpolarized (depolarized) band in agreement with experiments (Fig. 3). The outer current has a characteristic M-shape, observed in *Chara corallina*. Varying the nonlinear parameters, it is possible to obtain a M-shape only for the inner current or for both.

The stationary bifurcation is further characterized by a weakly nonlinear analysis performed in the vicinity of the threshold ( $k_c$ ;  $c_c$ ) [2]. An arbitrarily small expansion parameter  $\epsilon$  is introduced to separate the fast and slow scales in the problem. We define the slow independent variables  $X = \epsilon x$  and  $T = \epsilon^2 t$ , and Taylor-expand the

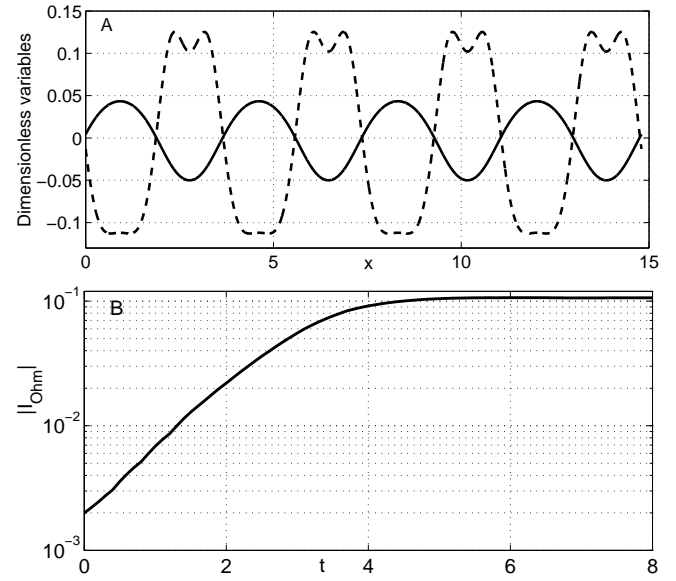


FIG. 3: Parameters are the same as in Fig. 2, with in addition  $\beta_2 = 0.25$ ,  $\beta_1 = 0.1$ ,  $\beta_2 = 0.1$  and  $\beta_3 = 5$ . A: The spatial stationary pattern is a modulation of the dimensionless membrane potential  $(V - V_0) = j V_0 j$  (—) and of the dimensionless ohmic part  $I_{ohm}$  (---) of the extracellular current. An hyperpolarized membrane potential  $(V - V_0) = j V_0 j < 0$  corresponds to an outer ohmic current (electric field) in agreement with experiments made with the vibrating probe. B: Temporal evolution of the extracellular current  $I_{ohm}$  at the position  $x = 12.5$ . The characteristic time is an ionic diffusive one.

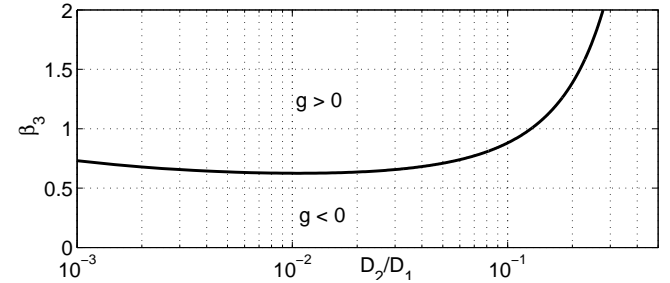


FIG. 4: The tricritical line  $g = 0$  separates domains in the reduced parameter space ( $D_2 = D_1$ ;  $\beta_3$ ) where the bifurcation is supercritical ( $g > 0$ ) and subcritical ( $g < 0$ ). The fixed parameter values are the same as in Fig. 3.

concentrations  $C_j$ , membrane voltage  $V$  and control parameter in powers of  $\epsilon$ . The resulting equations are then solved recursively for each power  $\epsilon^i$ . The solvability condition (Fredholm alternative) at third order provides the amplitude equation:

$$0 @_T A = A + \frac{2}{0} @_X^2 A - g A^2 j A; \quad (7)$$

where  $\epsilon = (c - c_c) = c_c$  is the reduced control parameter. The time and lengthscale  $\tau_0$  and  $\lambda_0$  of the pattern's slow modulations close to the bifurcation may also be derived directly from the dispersion relation (5):

$c_0^2 = \frac{1}{2} \frac{g_0^2}{g^2}$  and  $c_0^1 = c_0 \frac{g}{g_0}$  [2]. The coefficient  $g$  of the nonlinear term is a complicated function of the physical parameters. The bifurcation is supercritical (resp. subcritical) for positive (resp. negative) values of  $g$ . In the idealized case described here, and for typical parameter values, a tricritical line  $g = 0$  separates the two types of bifurcation in parameter space (see Fig. 4).

In conclusion, we established that a spatially homogeneous membrane voltage is linearly unstable if the co-transporters play a role in the control of the electrophysiological properties of a cell. The natural stationary pattern is a transcellular current bearing various ionic species. As opposed to many other scenarios leading to spatiotemporal pattern formation in ionic currents [1, 11, 12], a

negative differential conductance is not required. A necessary ingredient is the slow intracellular diffusion of one of the two ions translocated by the co-transporter. Interestingly, this is often the case in experiments. This mechanism may explain how a cell can uptake an essential nutrient at precise locations: in *Chlamydomonas*, methionine enters at the tip during apical growth.

We thank P. Pelcé for useful discussions. We wish to acknowledge the support of "ACIPhysico-chimie des systèmes complexes" (France), the Fonds National de la Recherche Scientifique (Belgium) and the Communauté Française de Belgique-Action de Recherches Concertées (Belgium).

- 
- [1] For a review, see Chaos 8, 1 (1998).
  - [2] M. C. Cross and P. C. Hohenberg, Rev. Mod. Phys. 65, 851 (1993).
  - [3] N. A. R. Gow, Adv. Microb. Physiol. 30, 89 (1989).
  - [4] For numerous examples of patterns of transcellular currents and a large bibliography, see [www.mbledu/labs/BioCurrents/Databases.html](http://www.mbledu/labs/BioCurrents/Databases.html)
  - [5] Pattern formation of transcellular ionic currents could also result from a Turing instability. However, contrary to the two other mechanisms, experimental evidence is still lacking.
  - [6] P. Fromherz and W. Zimmermann, Phys. Rev. E 51, R1659 (1995).
  - [7] P. Fromherz, Proc. Natl. Acad. Sci. 85, 6353 (1988).
  - [8] M. Leonetti and E. Dubois-Violette, Phys. Rev. E 56, 4521 (1997).
  - [9] S. C. Kramer and R. Kree, Phys. Rev. E 65, 051920 (2002).
  - [10] Experiments on the effect of electric fields on clustering of Acetylcholine receptors proves the relevance of the Fromherz mechanism at scales less than 50 microns. However, the large characteristic time predicted for patterns of larger wavelengths, such as observed in Chara corallina, is not consistent with experiments.
  - [11] M. Leonetti and E. Dubois-Violette, Phys. Rev. Lett. 81, 1977 (1998).
  - [12] M. Leonetti, E. Dubois-Violette and F. Homble, Proc. Natl. Acad. Sci. 101, 10243 (2004); and references therein.
  - [13] Contrary to excitable cells such as neurons and cardiac cells, a mismatch between the diffusive properties of the relevant ions inhibits (in a domain of parameters) the electrical instability at the origin of action potential and drives a diffusive linear instability.
  - [14] L. Limozin, B. Denet and P. Pelcé, Phys. Rev. Lett. 78, 4881 (1997).
  - [15] D. L. Kropf, M. D. Lupa, J. H. Caldwell and F. M. Harold, Science 220, 1385 (1983).
  - [16] F. M. Harold, in Tip growth in plant and fungal cells, ed. I. B. Heath (Academic Press, 1990) 59.
  - [17] As opposed to [11, 12], voltage-gated channels are not involved here. See also [10].
  - [18] For antiports,  $n + D_1 z_2 = D_2 z_1 < 0$  is replaced by  $n - D_1 z_2 = D_2 z_1 < 0$ . The two necessary conditions are  $D_1 > n D_2 \frac{z_1^2}{z_2}$  (unchanged) and  $z_2 = z_1 > 0$  (often fulfilled by antiports).
  - [19] For example, it is well established that the diffusion constant of the calcium ion is then reduced by at least a factor 100.
  - [20] D. L. Kropf, J. Cell Biol. 102, 1209 (1986).